PRODUCTION AND MAINTENANCE OPTIMIZATION OF SOLAR ENERGY USING MACHINE LEARNING TECHNIQUES

Aisha Sa'ad[1,2], Aimé C. Nyoungue[2], Zied Hajej[2], Mary Samuel[1], Abdulazeez Haruna[1], and Sani Umar Muhammed[1]

[1] Department of Mechanical Engineering, Nigerian Defence Academy, Kaduna, Nigeria.
[2] LGIPM, Université de Lorraine, Metz, France.

Corresponding Authors E-mail: a.saad@nda.edu.ng,

Abstract

In this paper, an optimal integrated production - maintenance strategy for a solar power plant, is presented. An optimal maintenance cost model applied to solar power plant with the aim of simultaneously maximizing a plant reliability and minimizing a maintenance cost was developed. The maintenance strategy is a combined priority imperfect/selective maintenance strategy, which selects the priority components for maintenance in order to reduce maintenance downtime. The goal of the paper is to simultaneously determine the optimal energy production and maintenance plan, characterized by the quantity of energy stored and the losses incurred when the energy demand is unmet. The strategy is to minimize the expected total cost of energy production (generation, storage, and shortage) as well as maintenance over a limited time horizon. Thus, determining the energy production economic plan, and the optimal number of maintenances to be performed that yields maximum reliability associated with the cost. A numerical example was presented to validate the developed model using Sokoto solar power plant in Nigeria as the case study.

Keywords:
Optimization, Support Vector Regression (SVR), Artificial Neural Network (ANN), Maintenance, Reliability.

1. INTRODUCTION

From the industrial revolution ages in early 19th century, the use of fossil fuel increased tremendously for energy generation, either as electricity or mechanical energy for driving vehicles. The use of fossil fuel no doubt, is a nuisance despite its importance as the major dependable energy source. Due to its excess emission of carbon oxides as by-products, it increases the carbon footprint in the atmosphere,

thereby obstructing the global energy balance in the ozone layer. The resultant effect been a subject of high concern in the United Nations (UN) organization. Also, the ever-growing global economy and increase in energy demand, it is nearly impossible to rely solely on these fossil fuel resources for a long period. Since the beginning of discussions on ways to mitigate our ailing environment from the effect of fossil fuels, therefore, efforts have been made by nations especially those considered industrialized or first world nations to reduce their carbon emissions. Therefore, the search for alternate source of energy emerged with renewables receiving great attention. Renewables are safe with near zero carbon emission. Despite the efforts in reducing carbon footprint, fossil fuel remains the leading energy source till date (Renewable Energy Market Update - Outlook for 2021 and 2022, 2021). The world energy generation chart presented in figure 1 shows that fossil fuel contributes about 73% of the world energy sources with all other sources taking up the remaining 27% (International Energy Agency, 2021).

Renewable energy technologies like hydropower, wind power, biogas, and photovoltaic systems are more effective in the utilization of primary energy, particularly in developing nations (Opiyo, 2018). The term "developing nations" typically signifies urban-centric development, leaving rural areas significantly underdeveloped. Approximately one billion people reside in scattered remote regions across developing countries globally, caught in a challenging struggle between demographic pressures and developmental needs. The pursuit of an improved standard of living, coupled with sluggish opportunity growth in rural settings, has triggered a swift and substantial shift from rural to urban areas. Consequently, this has led to a rapid expansion of slum areas around major cities. Prioritizing the enhancement of basic living conditions, addressing energy demands, and fulfilling other essential needs in rural areas is imperative to mitigate these challenges.

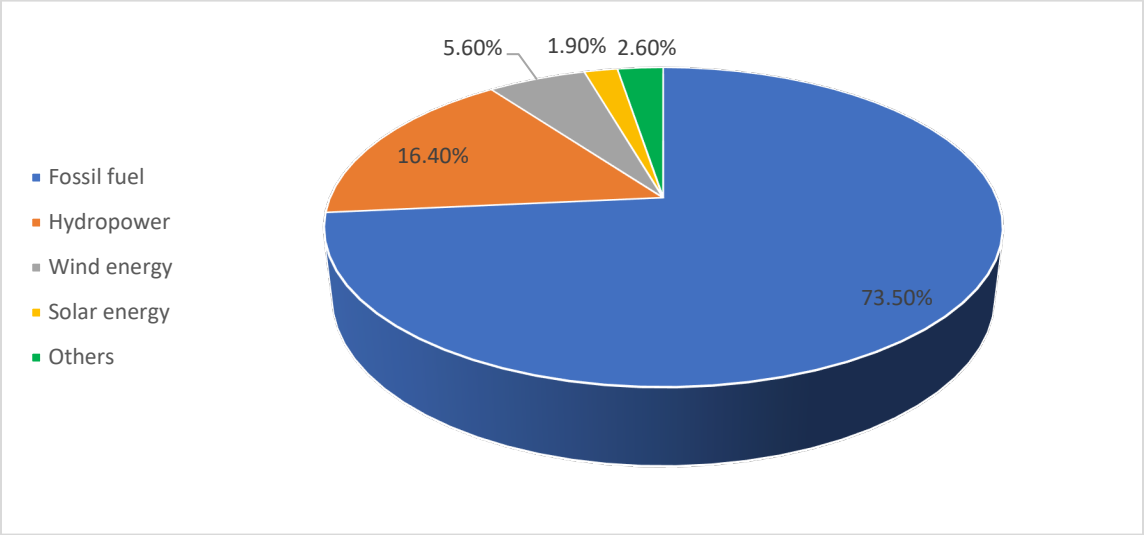

Effective harnessing of renewable energy sources necessitates thorough and efficient planning to ensure energy availability, even when the sources generate less than the demanded amount due to their reliance on weather conditions. Numerous researchers have delved into studying and devising algorithms to assess the capacity of renewable generating units capable of providing

cost-effective and reliable energy through various methodologies (Zhou W. et al, 2010). In their model, (Borowy B.S. and Salameh Z.M., 1996) introduced an iterative method to ascertain the optimal number of generating and storage units in a self-sufficient PV/wind hybrid energy system. This involved considering wind turbines of various sizes and capacities, and for each turbine, determining the optimal combination of PV panels and storage units to meet demand at minimal cost. Additionally, (Diaf S. et al, 2007) developed a model to estimate the levelized cost of energy, appropriately sizing the generating units in a standalone PV/wind hybrid energy system. The authors emphasized the pivotal role of selecting an adequate battery storage system in cost minimization. Consequently, they explored five (5) different storage capacities to identify the optimal capacity ensuring reliability in the loss of power supply probability (LPSP) at an optimal cost.

Simulation was conducted to analyze the behaviour of several combinations of PV, wind turbines, fuel cells and battery storage systems. For the conditions analysed, it was concluded that the PV/WT system with battery bank has lower costs of energy than other configurations. Furthermore, the optimal solution for the electrification of Kavaratti Island in India was examined based on minimizing the cost of energy. (Hosseinalizadeh et al., 2016) It was discovered that PV wind system with batteries is the best option for reducing the cost of each kWhr of electricity. Additionally, (Maatallah et al., 2016) the economic and technical feasibility of a hybrid PV/wind system with batteries in Bizerte, Tunisia was investigated using Hybrid Optimization of Multiple Energy resources (HOMER) software. It was discovered that adding batteries to the hybrid wind/PV system reduces the net present cost by 85%. (Bahramirad et al., 2012) estimated the optimal capacity of energy storage system (ESS) in a microgrid system where the objective was to minimize the cost of investment of the ESS in addition to the levelized cost of energy (LCOE) of the microgrid where their constraint was the reliability of the grid represented by the loss of load expectation. They found that larger ESS capacities do not always have larger economic benefits where the optimal size of the ESS should be found to ensure the economic feasibility of the ESS.

The above cited works were performed by the conventional methodology (empirical, analytical, numerical, hybrid, etc.). Sizing PV-systems generally requires knowledge of the sites' weather data (irradiation, temperature, humidity, clearness index, wind speed, etc.) and the information concerning the selected site are available. However, these techniques could not be used for sizing PV systems in remote areas, where the required data were not available. In all of these, accuracy is achieved by using data from daily global irradiation series. Majority of these conventional approaches need long term meteorological data such as total solar irradiation, air temperature, wind speed, etc. for their operation. Therefore, when the relevant meteorological data are not available, these methods cannot be used, especially in remote areas. In order to overcome this situation, methods that are more recent have been developed for sizing the parameters for PV-systems based on AI (Artificial Intelligence)-techniques (Mellit et al., 2009; Sa'ad et al., 2020, 2022).

Energy production is generally associated with losses especially maintenance losses. To minimize these economic losses, (Wang et al., 2022) developed strategy for optimal cleaning of a PV system. The authors proposed a risk-taking tendency (RTT) factor to reduce the uncertainty in energy production forecasting to minimize economic losses of cleaning the system. In (Tanesab et al., 2018) also, PV cleaning solution was proffered considering different scenarios for dust accumulation on the PV panels and its effect on the PV production. However, the effect of maintenance time and its consequential energy and economic losses were not taken into account.

Therefore, to establish a balanced system which further minimizes the PV system losses, this work takes into account the maintenance downtime to maximize the system reliability while simultaneously minimizing the production and maintenance costs. Hence, a joint optimal production and maintenance plan was developed to determine the economic plan of energy production and the optimal number of preventive maintenances to be performed as well as its periodicity which minimizes the production and economic losses of a solar PV energy system.

This work has been organized thus; formulation of integrated maintenance strategy was developed in Section 2, where production and maintenance strategy of PV system was discussed. In Section 3, PV study was carried out while the resolution algorithm and model testing (Numerical example) were presented in Section 4. Finally, Conclusion was drawn in Section 5.

2. INTEGRATED MAINTENANCE STRATEGY PROBLEM

This subsection deals with the development of integrated production maintenance strategy for a solar power plant taking into account the production cost, storage and shortage costs in to the maintenance planning constrained to reliability, power production, and the service rate. Before proceeding with the maintenance strategy, we first establish the optimal production planning technique presented in the subsequent sub-sections.

2.1 Production problem formulation

In this section, the mathematical models of the production optimization problem techniques using support vector regression (SVR) and artificial neural network (ANN) is presented as follows:

2.1.1 Artificial Neural Network (ANN)

An ANN is an array network of uncomplicated processors called neurons. A typical ANN architecture is shown in Figure 2. The ANN consists of an input layer, one or more hidden layers and an output layer. Each layer engages numerous other neurons and each neuron in a layer is connected to the neurons in the adjacent layer with different numerical values known as the weights. These weights are the core processors for performing the neural computations for the output. Data fed into the input layer, pass through the hidden layers, and reach the output layer to make prediction. With the exception of the input layer, each neuron receives data from the neurons of the previous layer linearly weighted by the weight between the neurons. The neuron then produces its output by passing the summed signal through an activation function. For example, a total of P sets of training data is assumed to be available. Inputs of P (i_1, i_2,…i_p) are the learning features and are imposed on the input layer. The ANN is trained to respond to the corresponding target output vectors, Y (y_1,y_2,…y_n) at the output layer. The training continues until a certain stop-criterion is satisfied. Typically, training is halted when the average error between the desired and actual outputs of the neural network over the P training data sets is less than a predetermined threshold. The training time required is dictated by various elements including the complexity of the problem, the number of data, the structure of the network, and the training parameters used.

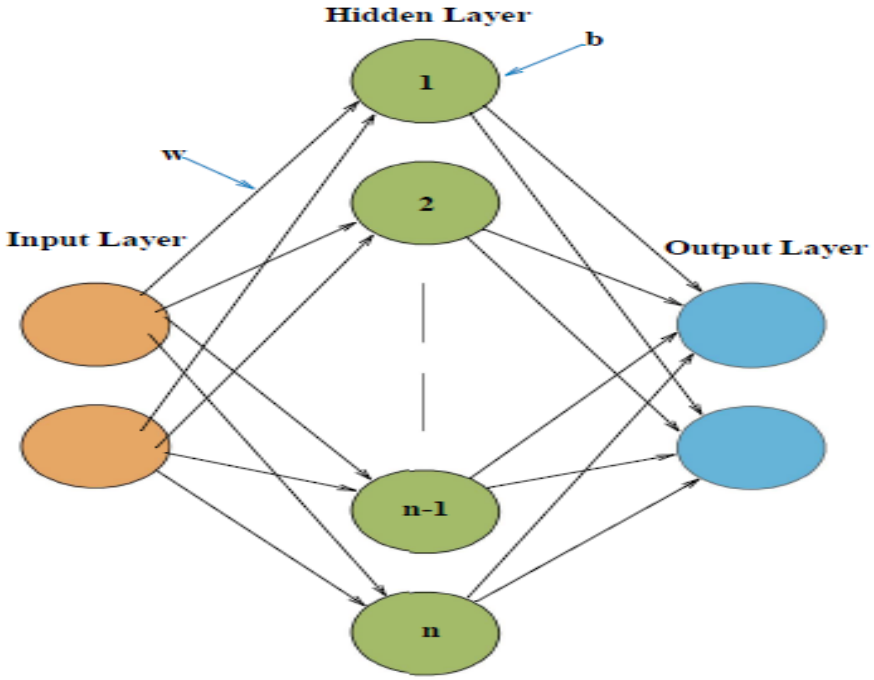

In this paper, the delta rule (Hanson, 1990) to train the ANN model using the neural network tool (nntool) in MATLAB 2021b was applied. According to the difference between the produced and target outputs, the network's weights ($w_{i,j}$) were adjusted to reduce output error. In case of high error, the output layer is propagated backward to the hidden layer until it reaches the input layer, adjusts the weights and recomputes the output. This process is known as the backward propagation. For the purpose of this work, a model comprising of input layer with 2 features (temperature and solar irradiance), single hidden layer comprising of 10 neurons and a single output for predicting our power production were trained.

The output, from neuron i, was connected to the input of neuron j through the interconnection weight $w_{i,j}$, The input to neuron j is defined as:

$$k_{j,input} = \sum_{i=1}^{m} w_{i,j}x_i + b_{input} \qquad (1)$$

x_i is the i^{th} input node, $k_{j,input}$ is the input of the j^{th} hidden node, $w_{i,j}$ is the weight assigned to the i^{th} input node that is mapped to the j^{th} hidden node and b_{input} is the input layer bias.

The output from the hidden layer was activated by an activation function and in this case, the sigmoid function because of its adaptability with even complex data was selected. The output therefore was obtained as

$$k_{j,output} = f(k_{j,input}) \qquad (2)$$

$k_{j,output}$ is the output of the j^{th} hidden node while f is the activation function of the model expressed as $1/(1+e^{-x})$

Through the computations and mathematical manipulations, the output prediction from the ^{jth} hidden node of the hidden layer is

$$y_p = \sum_{j=1}^{n} k_{j,output} + b_{hidden} \qquad (3)$$

b_{hidden} is the hidden layer bias and y_p is the output of the model.

2.1.2 Support Vector Regression

The Support Vector (SV) is a nonlinear kernel-based machine learning technique used for regression as well as classification. The kernel functions as activation power which makes the model exhibit good prediction ability. It consists of creating or mapping training data into hyper-planes to vividly discriminate predictions from training data in the feature space as shown in figure 3 and this characteristic makes the support vector deal efficiently with nonlinear regression problem.

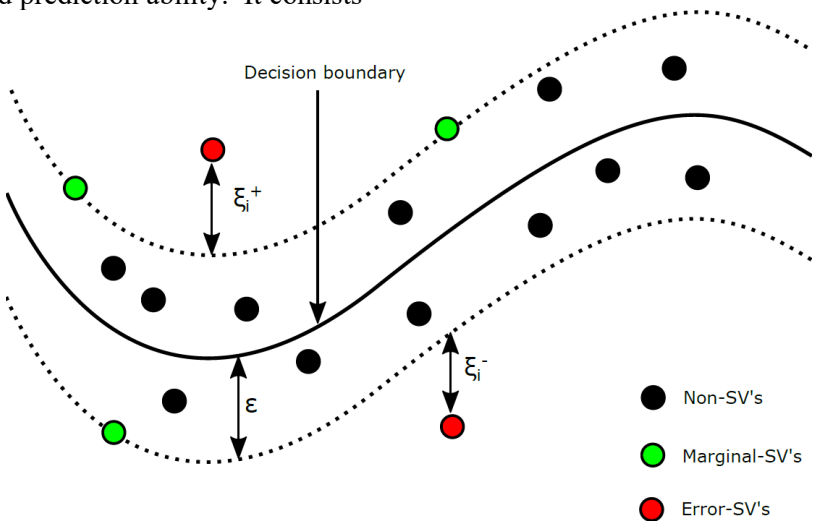

Figure 3: SVR architecture

Given a set of data points represented by $\{x_i, y_i\}_i^n$ whereby x_i is the input space vector from the sample, y_i is the target value and n, is the total sample size. A support vector machine output prediction is calculated in the following form:

Where φ is the transfer function, x is an input data point. w is a normal vector and b is a scalar and they are estimated by minimization of regularized risk function by introducing regularized risk function solved as (Cortes & Vapnik, 1995).

$$\text{minimize } L_P = \frac{1}{2}\|w\|^2 + C\sum_{i=1}^{l}(\xi_i + \xi_i^*) \quad (5)$$

$$\text{Subject to} \quad \begin{cases} y_i - \varphi(x_i) - b \le \epsilon + \xi_i \\ \varphi(x_i) + b - y_i \le \epsilon + \xi_i \\ \xi_i,\ \xi_i^* \ge 0 \quad i = 1,2,\dots n \end{cases}$$

where $\frac{1}{2}\|w\|^2$ represents the regularization term, y_i is the i^{th} target and C is the error penalty factor used to control the trade-off between the regularization term and empirical risk, ϵ is the deviation threshold of the function f, and ξ_i is the slack error that guarantees the solution by coping the in-feasible constraints and *n* is the number of elements in training data sample.

Equation 4 can be solved by introducing Lagrange multiplier and optimality constraints, hence obtaining a generic function given by

$$f(x) = \sum_{i=1}^{n}(\beta - \beta^*)K\left(x_i, x_j\right) + b \quad (6)$$

Where $K\left(x_i, x_j\right) = \varphi(x_i), \varphi\left(x_j\right)$ and the term $K\left(x_i, x_j\right)$ is called the kernel function, which is a product of the two vectors x_i and x_j in the feature

space $\varphi(x_i)$ and $\varphi(x_j)$ respectively. This product associates each pair of vectors in the space with a scalar quantity known as the inner product of the vectors. Inner products allow the rigorous introduction of intuitive geometrical notions such as the length of a vector or the angle between two vectors (Olatomiwa et al., 2015). The main purpose of SVMs is to carry out data correlation via non-linear mapping. Kernel methods enables it to operate in a higher dimensional feature space without ever computing the coordinates of the data in that space, but rather by simply computing the inner products between the metaphors of all pairs of data in the feature space. This operation is often computationally cheaper than the explicit computation of the coordinates. This approach is known as a direct computation method of a kernel function, denoted by K. The results obtained in the higher-dimensional feature space correspond to the results of the original, lower-dimensional input space.

There are four basic kernel functions provided by SVM, namely, linear, sigmoid, polynomial, and radial basis functions. But over the years, Radial Basis Function (RBF) has been proven to be the best kernel function due to its computationally efficiency, simplicity, reliability, ease of adaptation to optimization and other adaptive techniques as well as its adaptability in handling parameters that are very complex (Yang et al., 2009). RBF kernel function only needs the solution of a set of linear equations instead of the lengthy and computationally demanding quadratic programming problem for its training. The RBF kernel function is defined as:

$$K(x_i, x_j) = e^{\gamma\|x_i - x_j\|^2} \quad (7)$$

where xi and xj are vectors in the input space, i.e. vectors of features computed from training or test samples.

The three parameters associated to RBF Kernels are γ, ϵ and C. The accuracy of SVM model is principally dependent on model parameter selection. In our work we used the default value of e = 0.1 which seemed to perform well. To select user-defined parameters (i.e. γ, ϵ and C), a large number of trials were carried out with different combinations of C and γ for the radial basis function kernel. It is worthy of mention that SVRs are effective with limited samples which also minimizes structural risks of the regression problem. Furthermore, SVRs have a wide application range such as solar irradiance prediction (Voyant et al., 2017), energy generation predictions (Sa'ad et al., 2020), anomaly detection (Harrou et al., 2021) and road traffic prediction (Zeroual et al., 2021).

2.1.2 Power production planning optimization

The power system considered in this work is solar panels and battery bank. Battery is not a generating unit but an energy storage system that supplies the load when there is lack of electricity and stores the surplus when the power generated exceeds the load. In some cases, where there is shortage of energy to satisfy the demand, out-sourcing was considered, therefore, this design considered the cost of shortage in the optimization of the system. Optimization process can be defined as the finding values of variables that minimize or maximize an objective function and satisfy the constraints. The optimization problems are centred on three main factors which are: i) objective function which is to be minimized or maximized, ii) a set of unknown variables that have effect on the objective function, and iii) a set of constraints that allow the unknown to take on certain values. In this work, the optimal cost index of the system C_{sys} is considered through the following optimization problem

$$\text{Mi}C_{sys}(N_{PV}, C_b) \quad (8)$$

Subject to:

$$N_{pv} * Ppv(t) + V_b * SOC(t) \geq P_L(t)$$

$$AEC_{min} \leq AEC(t) \leq AEC_{max}$$

There are various ways to calculate system costs (Bernal-Agustín et al., 2006; Dufo-López et al.,

2007). In this paper, we adopt the system life cycle cost consisting of the initial capital cost and the operational costs. This capital cost comprises of cost of purchasing and installing the units while the operational costs which comprises of the unit cost of generation 1kW of energy, unit cost of storing 1kW of energy and unit cost of shortage expressed by the following equations (Li et al., 2012).

$$C_{system} = C_{cap} + C_{ope} \quad (9)$$

$$C_{cap} = \sum_{t=1}^{H} N_{pv}(t) * C_{pv} + C_b(t) * C_{bat} \quad (10)$$

$$C_{ope} = C_{t1} + C_{t2} + C_{t3} \quad (11)$$

The operational cost characterized by the costs of production (C_{t1}), cost of storage (C_{t2}) and cost of shortage (C_{t3}). These costs are evaluated as follows:

$$C_{t1} = \sum_{t=1}^{H} \left(C_p \times \sum_{j=1}^{N_{pv}} P_{js}(t) \right) \quad (12)$$

$$C_{t2} = \left(C_s^{+} \times \Delta t \times \sum_{t=1}^{H} \left(SOC(t) \times 1_{SOC(t)>0} \right) \right) \quad (13)$$

$$C_{t3} = \left(C_s^{-} \times t \times \sum_{t=1}^{H} \left(SOC(t) \times 1_{SOC(t)<0} \right) \right) \quad (14)$$

With the storage condition on the battery's state of charge being

$$1_{SOC(t)>0} = \begin{cases} 1 \text{ if } SOC(t) > 0 \\ 0 \; otherwise \end{cases}$$

and that of shortage condition on the battery's state of charge being

$$1_{SOC(t)<0} = \begin{cases} 1 \text{ if } SOC(t)) < 0 \\ 0 \; otherwise \end{cases}$$

Here, C_p is the cost of production per unit kW, C_s^{+} is the cost storage per unit kW, C_s^{-} is the cost of shortage per unit kW and P_k is the total power generation within production period k. We assume that the quantity produced in period k is added to the inventory at the end of the period which satisfies the demand P_L. Accordingly, the inventory evolves as shown in Figure 4 below

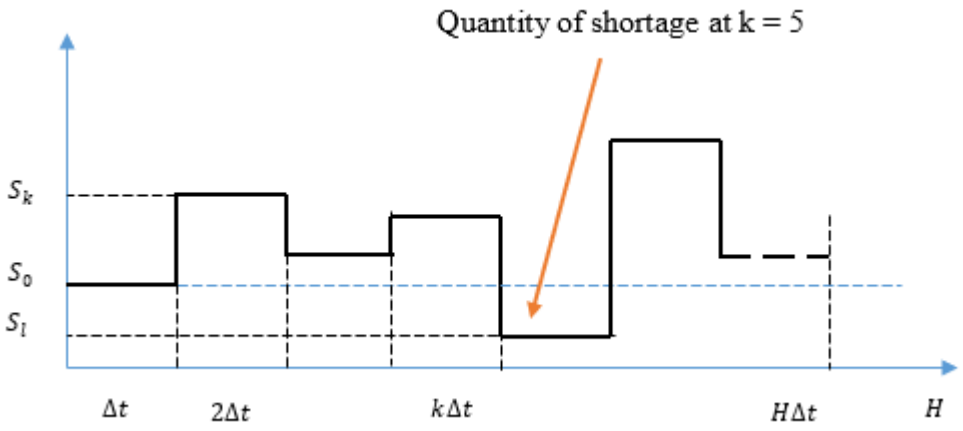

Figure 4: Evolution of storage inventory

2.1.3 Storage sizing problem

The battery storage behaviour is characterized by its state of charge (SOC) (Piller et al., 2001). The SOC depends on the past data and the power in the battery system which is the difference between the generated power $P_G(t)$ and the

power load demand $P_L(t)$ at every time instance t. Therefore,

$$SOC(t) = SOC(t-1) + \frac{P_G(t)-P_L(t)}{V_b.TC_b} \quad (15)$$

Given that

$$P_G(t) = \sum_{t=1}^{H} N_{pv} \times P_S(t) \quad (16)$$

Where V_b *and* C_b are the battery voltage and capacity respectively.

To ensure good performance of the battery bank, a new concept of cycle invariance criterion is introduced (Li et al., 2012). The cycle invariance criterion is such that, the battery SOC returns to its initial state $SOC(t_0)$ at the end of each production period which implies that

$$SOC(t) = SOC(t-1) \quad (17)$$

This criterion helps in proper sizing to determine the number of panels required, hence equation 17 is remodelled into

$$\sum_{t=1}^{H}(N_{pv} \times P_S(t) - P_L(t)) = 0 \quad (18)$$

Therefore,

$$N_{pv} = \frac{\sum_{t=1}^{H} P_S(t)}{\sum_{t=1}^{H} P_L(t)} \quad (19)$$

After N_{pv} is determined, the battery capacity is obtained by calculating the energy flowing into and out of the battery bank $P_b(t)$ at time t by

$$P_b(t) = P_G(t) - P_L(t) \quad (20)$$

At present, the total battery capacity (TC_b) is undetermined, then we let $AEC(t)$ denote the available energy capacity of battery bank at t expressed as:

$$AEC(t) = AEC(t_0) + \sum_{t=1}^{H} \frac{P_b(t)}{V_b} \quad (21)$$

We assume that the initial condition $AEC(t_0) = 0$ which means the battery is empty at the initial condition. This causes the energy in the battery bank to be less than zero (0) which is not technically feasible. To overcome this, a suitable initial condition is proposed such that the $AEC(t)$ at each period is characterized by the SOC variation which is expressed as

$$AEC(t) = SOC(t).C_b \quad (22)$$

To determine the total battery bank capacity TC_b over a finite time horizon H, the TC_b must satisfy the following condition in order not that the battery capacity does not become negative

$$TC_b \geq AEC_{max} - AEC_{min} \quad (23)$$

where

$AEC_{max} = \max(AEC(t))$ and $AEC_{min} = \min(AEC(t)) \quad \ni t = 1 \dots H$

If $P_G(t) > P_L(t)$, the battery becomes in a charging state and if otherwise when $P_G(t) < P_L(t)$, the battery gets into a discharge state. The $AEC(t)$ of the battery during the charging and discharging states are expressed in the following form:

$$AEC(t) = AEC(t-1).(1-\sigma) + \left(PG(t) - \frac{PL(t)}{\eta_{inv}}\right).\eta_{bat} \quad (24)$$

$$AEC(t) = AEC(t-1).(1-\sigma) - \left(\frac{PL(t)}{\eta_{inv}} - PG(t)\right) \quad (25)$$

$\boldsymbol{\sigma}$ is the battery self-discharge rate given as 25% by the battery manufacturer, η_{inv} is the inverter efficiency considered as constant, (92%) and η_{bat} is the battery efficiency is set to 1 during discharge process and 0.65 during charge ng state. On another hand, to improve the battery efficiency, the battery energy flow within the battery must be limited within a certain range and then the maximum absorbable energy (Capata, 2011) must be considered as

$$TC_b \geq |P_b(t)|/V_b \ni t = 1 \dots H \quad (26)$$

Each battery cycle is characterized by its depth of discharge (DOD) so as to guarantee the battery cycle and minimize deep cycle, which means that the amount of capacity withdrawn from a battery expressed as a percentage of its maximum capacity. Therefore, the allowable DOD must be taken into account so as to extend the working life of the battery. Therefore, the TC_b is maximum of the combination of equation 23 and 26 becomes:

$$TC_b = max\left(\frac{(AEC_{max} - AEC_{min})}{DOD}, |P_b(t)|/V_b\right)/ \quad (27)$$

2.1.4 Service rate

Due to the volatile nature of solar energy, it is not always easy to plan simple activity because the sources are random and stochastic. Solar power generation therefore is a challenging task that requires an understanding of the functionality and reliability of solar panels and its components to ensure customer satisfaction. Facing all these tasks at the same time requires careful study and planning in advance. To solve the problem therefore, we propose a model to carefully plan the energy production considering the production rate and a level of storage. The objective of the production policy is to optimize the production system by minimizing the costs linked to the production cycle over the finite time horizon H.Δt.

As for the battery storage system, it provides the electric power to supply the load demand when there is a power shortage from production and stores the surplus energy when the generated power exceeds the load. In this section, we mainly focus on the costs related to the production and storage of energy. It is possible to satisfy the demand during each period k in different ways:

- Using the quantity produced during period k;
- Using the quantity stored in the battery if sufficient.
- When these are not sufficient, we consider buying from outside (incurs cost due to loss).

In this context, it can be said that storage is essential to ensure the smooth demand supply. This leads us to talk about an important concept in the industrial field, which is the concept of service level. In business, service level is a performance metric used to measure customer service satisfaction in supply organizations. In the manufacturing industry, the service level is almost the same defined and considered as a major factor used to describe business performance. It measures the ability of an industry to meet the demand and requirements of its customers in a timely manner. This service level can be expressed in several terms:

- Probability of failure;
- Estimated number of failures;
- Time elapsed between successive cases of failure;

In this work therefore, the first method consisting in expressing the service rate as the probability of non-failure between two successive periods was considered. The service rate can be illustrated as:

$$prob(S(k)>0)>\theta \quad (28)$$

With θ minimum level of customer satisfaction (service level threshold)

3 3. Solar PV maintenance strategy: maximizing reliability

This section discussed the photovoltaic system, its main components and the types of failure occurring on each component. It also highlights the important functions of the components. A typical photovoltaic plant is a complex system composed of different electronic devices predominantly photovoltaic modules and inverters as shown in figure 5. The photovoltaic modules are usually either connected in series, in parallel or a combination of both. When connected in series, it improves the voltage while in parallel improves the current. Different series are connected in series to improve the intensity to form the photovoltaic field. As the output of the photovoltaic field is a direct current, the series are connected via DC wires to the inverters which convert the output to an alternative current (AC).

The output of the inverters then feeds the load via AC wires.

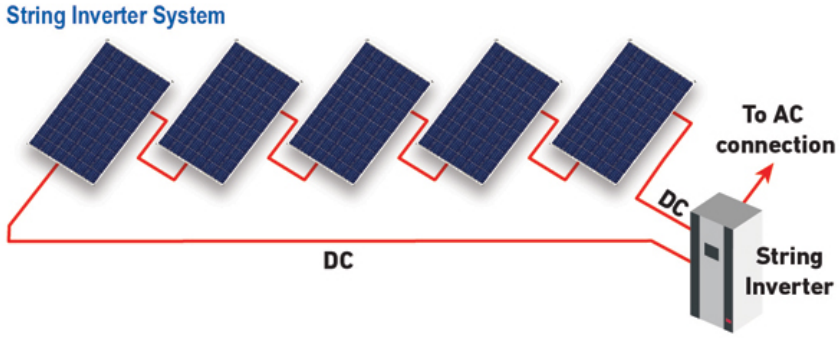

Figure 5: A PV field layout

The main components of a PV system are:

i. **Panels:** These are the large and most visible part of the PV system. It comprises of solar cells connected in series to be able to generate substantial amount that can be able to power a bulb or charge phone. These cells are made up of semiconductor crystalline silicon particles which can be either monocrystalline or polycrystalline in nature. When sunlight hits a solar cell, the electrons in the semiconductor get energized and create an electric field in the cell causing electric current to flow from cell to cell. The panel generates direct current (DC) which are non-consumable.

ii. **Inverter:** This is an important component in the PV system because its main function is to convert a DC current to a consumable form known as an alternating current (AC) used in residential and commercial properties.

iii. **Battery:** This component is used to store excess unused energy.

In order to determine the reliability of the system as proposed in this work, we first have to define the reliability of the system based on the reliabilities of the above-mentioned main components expressed as the following:

(i) Reliability estimation

We must say that the reliability of the PV system is complex and contains a large number of sub-assemblies that may be connected in series, parallel or even a combination of both. When the sub-assemblies are connected in series, the overall system will be interrupted in case of failure of one sub-assembly. However, all sub-assemblies must fail in order to interrupt the overall system in the parallel connected system. For components associated in series, the reliability of the group is assumed to be the product of each component reliability as shown in eqn 29:

$$R(t) = R_1(t).R_2(t) \dots R_n(t) = \prod_{i=1}^{n} R_i(t) \quad (29)$$

The PV system considered in this work is composed of different components associated in series. Therefore, unreliability function Q is used to define the reliability of the group expressed in eqn 30. The unreliability of the equipment is expressed as the product of each component's unreliability (Mahani et al., 2019):

$$Q(t) = \left(1 - R_1(t)\right).\left(1 - R_2(t)\right) \dots \left(1 - R_n(t)\right) \quad (30)$$

Therefore, the reliability is remodelled as in eqn 31

$$R(t) = 1 - \prod_{i=1}^{n}(1 - R_i(t)) \quad (31)$$

For each of the components considered, the reliability of the equipment has various failure causes assumed to be the product of the reliability

functions established for each failure cause expressed below

$$R(t) = \prod_{i=1}^{n} R_{cause\,i}(t) \quad (32)$$

Extracted from the work of *(Sa'ad et al., 2021)* photovoltaic field, DC Wires, inverters and AC Wires are the most sensitive components whose reliability has a major impact on the system. Therefore, in this work, we considered the mentioned components arranged in Series as expressed in equation 33.

$$R_{system}(t) = R_{PVfield}(t).R_{DC\,Wire}(t)^{n_{DC\,Wires}}.R_{Inverters}(t)^{n_{Inverters}} \quad (33)$$

The reliability of each of the subcomponents is expressed below:

a) Photovoltaic Field Reliability:

Regarding the PV Panels, the components and possible causes of failure are: junction box, glass, bye-pass diode, cells, ribbons, hotspot, delamination, ribbons and interconnectors on the panels. There are also failures due to chemical reactions; corrosion and discoloration. The panel reliability therefore was determined by evaluating the reliability of the panel compoennt and that of the failure cause which can be expressed as

$$\boldsymbol{R_{panel}(t) = R_{panel\,components}(t).R_{causes}(t)} \quad (34)$$

Using the exponential law, the PV panel reliability are expressed as:

$$R_{panel}(t) = e^{-(\lambda_{junction\,box}+\lambda_{bypass\,Diode}+\lambda_{cells}+\lambda_{ribons}+\lambda_{interconnectors})\cdot t} \cdot e^{-(b_{discoloration}+b_{corrosion}).t+a_{discoloration}+a_{corrosion}} \quad (35)$$

b) DC/AC wires Reliability:

The DC Wires and the AC Wires reliability functions are of the same form, as such they are treated in a similar way. The Wires have two failure causes; cut and corrosion. For each cause, the reliability function has a different form,

$$\boldsymbol{R_{wire}(t) = R_{cut}(t).R_{corrosion}(t)} \quad (36)$$

But the general reliability for both wires is with the exponential function:

$$R_{wire}(t) = (1 - C_{corrosion-wire}.t^{a_{corrosion-wire}}) \cdot e^{-\lambda_{cut-wire}\cdot t} \quad (37)$$

c) Inverter Reliability:

The inverter is a complex and expensive component of a photovoltaic system. The main causes of failure in inverters are mainly design problems, manufacturing defects and poor management practices *(Realini, n.d.)* even though temperature and humidity can affect the functionality of the inverter. Thus, low inverter reliability contributes to an unreliable system and a loss of confidence in the renewable technology. The reliability function described by an exponential distribution often characterized by failure rate (λ) and is expressed as in the equation below:

$$R_{inverter}(t) = e^{-\lambda_{inverter}t} \quad (38)$$

Overall PV system reliability is expressed below

$$R_{pvplant}(t) = \left(1 - \left(1 - \left(e^{-(\lambda_{junction\,box}+\lambda_{junction\,box}+\lambda_{cells}+\lambda_{ribons}+\lambda_{interconnectors})\cdot t} \cdot e^{-(b_{discoloration}+b_{corrosion}).t+a_{discoloration}+a_{corrosion}}\right)^{n_{panels}}\right)^{n_{series}}\right) \cdot \left((1 - C_{corrosion-DC}.t^{a_{corrosion-DC}}) \cdot e^{-\lambda_{cut-DC}\cdot t}\right)^{n_{DC\,Wires}} \cdot \left((1 - C_{corrosion-AC}.t^{a_{corrosion-Ac}}) \cdot e^{-\lambda_{cut-AC}\cdot t}\right)^{n_{AC\,Wires}} \cdot \left(e^{-\lambda_{inverter}\cdot t}\right)^{n_{inverter}} \quad (39)$$

For more explanation on the mathematical explanation, see the appendix

(ii) Optimization of maintenance cost

The mathematical model for minimizing the maintenance cost of the system over the production horizon is expressed below:

$$min\, C = min \sum_{k=1}^{H} \left(\underbrace{C_p.P_k + C_s.S_k + C_l.S_l}_{production+,storage+shortage\ costs} \right) + \underbrace{C_{post}}_{loss\ cost} \quad (40)$$

With

$$C_{post} = C_{sell} \times \frac{\sum_{k=1}^{H} P_k \times (\mathrm{T_{maintenance}(N)})}{H} \quad (41)$$

With the $\mathrm{T_{maintenance}(N)}$ characterized by the maintenance actions duration is expressed by the following equation:

$$\mathrm{T_{maintenance}(N)} = \underbrace{\sum_{j=1}^{N} \sum_{i=1}^{NC} [\mu_{P_i} \times m_i(j)]}_{\text{preventive maintenance duration}} + \underbrace{\mu c \times \varphi(N)}_{\text{corrective maintenance duration}} \quad (42)$$

subject to

$$0 < P_k < P_{max}$$

$$(P(S(k) > 0) > \theta$$

$R_{PV}(t) > R^*$ for the PV system

$$m_i(j) = \begin{cases} 1 \ if\ the\ i^{th}\ component\ is\ to\ be\ replaced \\ 0 \qquad\qquad otherwise \end{cases}$$

where S_k is the quantity of energy stored in the battery and S_l is the quantity of energy lost that needs to be outsourced in order to satisfy the demand and P_k is the amount of electricity produced during period k. $C_p, C_s, C_l, C_{post}\ and\ C_{sell}$ are the cost of production, cost of storage, cost of shortage, cost of post-production and cost of selling for 1 unit of electricity respectively. While $\mu_c, \mu_p, N\ and\ \varphi(N)$ are associated with the maintenance; and are respectively preventive maintenance time, corrective maintenance time, total number of maintenances and average number of failures for considering any particular N and

$i \in \{1,2, \ldots \ldots NC,\}$: i^{th} Subcomponent;

NC: Number of subcomponents;

$j \in \{1,2 \ldots . \mathrm{N}\}$: Maintenance period

$m_i(j)$ is a binary vector string for the components such that it equals 1 if the component is to be replaced and 0 if maintenance is not to be performed. The average number of failures is expressed as

$$\varphi(N) = \sum_{k=0}^{N-1} \left[\int_{k.T}^{(k+1).T} \lambda_{PVk}(t)\ dt \right] + \int_{N.T}^{H.\Delta t} \lambda_{PVk}(t)\, dt \quad 43$$

$$\lambda_{PV,k}(t) = \frac{-\frac{dR_{PV,k}(t)}{dt}}{R_{PV}(t)} \quad 44$$

.

4. Resolution algorithm and case study

Towards achieving the objective of this research work, which is determining optimal number of preventive maintenance sessions (N* ∈ {1… N}), we therefore developed an algorithm based on the following simple numerical procedure shown on Figure 6. We built the algorithm to select the components whose criticality falls under the set threshold of reliability, and customer satisfaction of service rate. First, we calculate the power production using both machine learning techniques; ANN and SVR techniques which are used as the input for the maintenance strategy. For each value of N, the algorithm computes the reliability and selects the critical components for maintenance while also respecting the minimum service rate during computation of the maintenance cost. The N* will correspond to the cheapest maintenance cost C* having the highest reliability.

The maintenance strategy adopted is perfect maintenance with minimal repair at failure as explained as follows; Solar energy components maintenance is carried out every k.T period (1,2...kN). Preventive maintenance actions are considered as replacements allowing to restore the system to a new condition termed 'As Good as New'. After a perfect maintenance action, the distribution of lifetimes and the function of the

failure rate are the same as those of a new unit. When a failure occurs between two successive preventive maintenance actions, a minimum repair is then carried out. In this strategy, it is assumed that the maintenance time and cost are not negligible. The change in the amount of energy produced by the solar PV during the production horizon H acts on the failure rate of the system. Since all the solar panels have the same power ratings in this work, we assume that they have the same power output, the maintenance planning is considered for one (1) solar.

To demonstrate the viability of the developed algorithm, Sokoto State solar power plant from Nigeria was used as the case study. Sokoto is a state in the north western part of the federal republic of Nigeria located on $13° 44'N$ and $5° 02'E$. It is characterized by dry Sahel savannah and sandy hills. The state is usually hot and arid where annual mean temperature is about 28.3 °C, and maximum daytime temperature of about 40 °C. It has daily average sunshine hours of 12 hours 53 minutes and daily average solar irradiance of 258.51 W/m^2 all year-round, thus making the location suitable for harnessing solar energy Adejumo et al., (2017). The periodic average solar irradiance and average temperature over the 12 periods (months) is presented on figure 7 and 8. The considered case study is the 55MW solar power plant operating where weo aim to consider the power plant as stand-alone expected to supply energy the host community of Yabo town and its environs. Relative humidity, temperature and solar irradiance data for 2 years from 2018 – 2020 were collected and used to train our models. For the purpose of this work, we consider only the host community of Yabo town for the analysis.

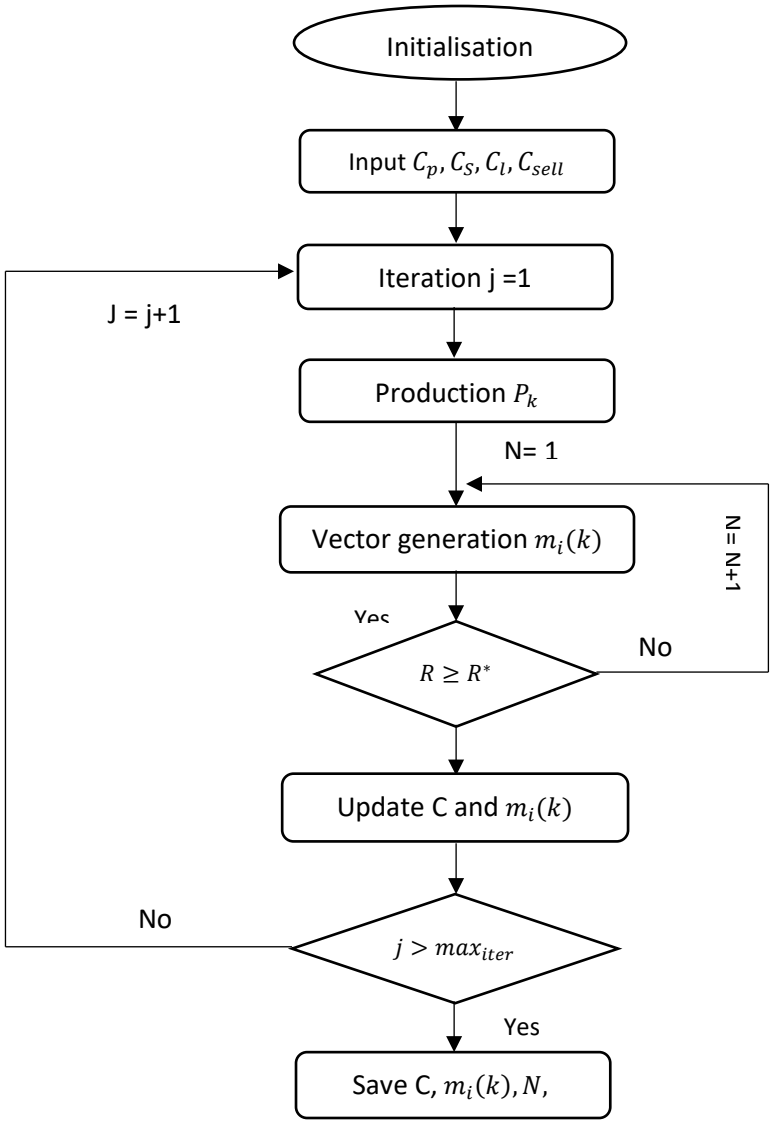

Figure 6: Maintenance algorithm

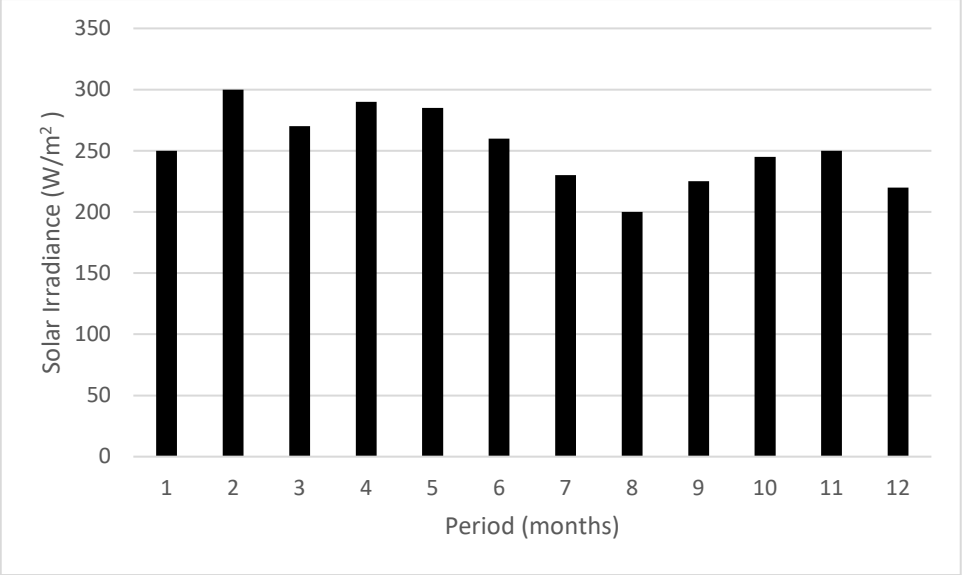

Figure 7: Solar irradiance of Sokoto

In Nigeria, it is estimated that the cost of energy production and storage from the solar power plant is 12 NGN and 15 NGN respectively. NGN is the Nigerian currency known as Nigerian Naira (1NGN = $ 0.0024). When load demand is not met and energy has to be sourced from the grid, the cost of this shortage is obtained at 25 NGN.

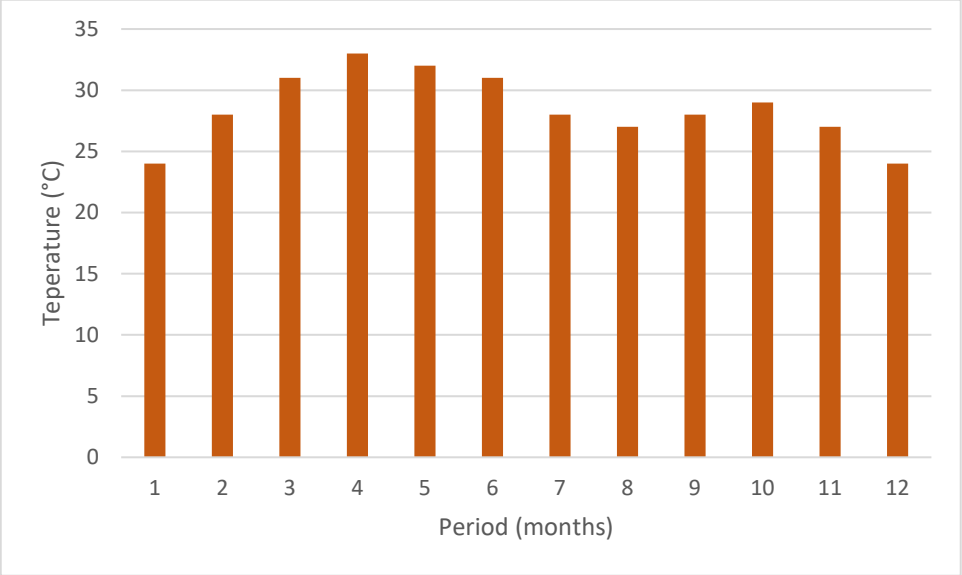

Figure 8: Temperature of Sokoto

A polycrystalline PV module (AE215P6-72) was found suitable for this site having considered its characteristics. It consists of 72 cells with a 30-year performance life span. The

characteristics of the panel are shown on Table 1, while the battery characteristics are presented on Table 2.

Table 1: Solar panel characteristics

Parameter	Value
Nominal Power (W)	215
Max power voltage (V)	37.18
Max power current (A)	9.28
Module efficiency (%)	
Operating temperature (°C)	
NOCT (°C)	
Module dimensions (mm^2)	1956 x 992

Table 2: ALFA-012125A Li-ion battery

Nominal charge (A)	Capacity (Ah)	Voltage (v)	Energy Stored (Watt-hour)	Cycle Life (cycles)
20	125	12	1500	2000 +

The average estimated load demand from the case study (Yabo town) is presented on Figure 9. Considering the customer service rate, we have chosen a threshold of 0.8 for this algorithm development.

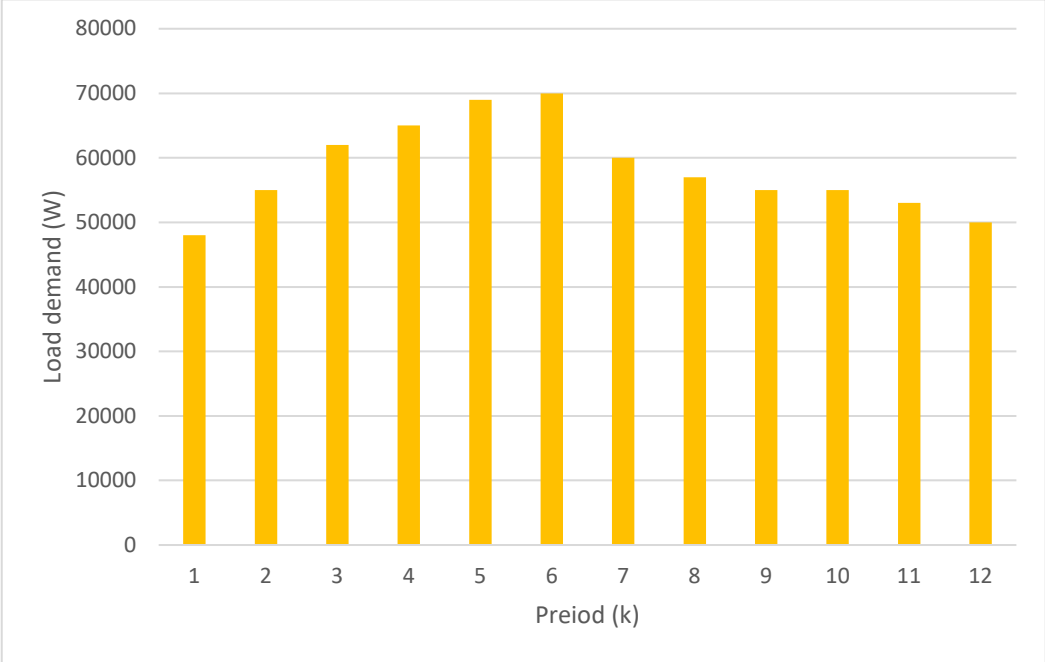

Figure 9: Average load characteristics of the Yabo town (Sokoto State, Nigeria)

5. Results and discussion

5.1 Production planning result and discussion

Production planning considering the customer satisfaction rate as constraint in order to be able to improve production from the system has been successfully conducted. Having done that, the results obtained with the developed algorithm are presented on tables 3 & 4 for both ANN and SVR techniques. On Tables 3 and 4, the optimal production planning results from using machine learning approach (ANN and SVR) is presented. For the ANN method on Table 3, the optimal cost was forecasted to be 2.5246 x10^6 NGN, while the SVR approach presents an amount of 3.5150 x10^6 NGN as shown on Table 4. We could see that machine learning presents the minimal costs as compared with the theoretical method. This can be explained by the ability of the machine to easily learn from previous data and adapt to make a better prediction by adjusting the learning rates until minimal error is obtained. Among the two (2) methods, the ANN is seen to present the optimal minimal cost among the 2 methods.

Table 3: Optimal production plan using the ANN approach

Total Cost (NGN) = 2.5246 x10^6		
Period (k)	Generated power (x10^4 W)	Stored power (x10^3 W)
1	5.9223	1.0977
2	5.8062	2.8203
3	5.7191	4.9758
4	5.6610	6.4370
5	5.6901	8.0518
6	5.7191	1.2689
7	5.8062	1.8167
8	5.8352	3.4498
9	5.8062	3.1590
10	5.7772	0.8924
11	5.8352	5.4498
12	5.9223	8.2231

Table 4: Optimal production plan using the SVR approach

Total Cost (NGN) = 3.5150 x10^6		
Period (k)	Generated power (x10^4 W)	Stored power (x10^3 W)
1	3.6302	4.4370
2	4.7415	5.0259
3	5.7802	5.6220
4	5.9102	5.9090
5	5.6625	5.9337
6	5.9535	6.4046
7	4.6290	5.5371
8	3.9547	5.1045
9	4.3162	5.0684
10	5.0038	5.1996
11	4.5091	4.8491

12	4.0725	4.5928

Sensitivity analysis

Since we considered the customer satisfaction probability in our model, we decided to vary the service rate to 60%, 70%, and 90% in order to understand its influence on the production cost. The results of this variation are presented on Table 5 where we observe that production costs are seen to be increasing with increase in the customer service rate.

Table 5: Influence of service rate on production cost

Technique	Service rate (%)	Cost (x10^6 NGN)
ANN	60	1.3010
	70	1.4984
	80	1.5246
	90	1.6393
SVR	60	3.2988
	70	3.3910
	80	3.5150
	90	3.6000

5.2 Maintenance result and discussion

In this section, we present the maintenance analysis established. Table 6, presents the maintenance inputs for maintenance planning. Since our maintenance strategy is an imperfect/ selective strategy, the table shows the cost and time of reparation for each component such that only the cost associated with the selected component is chosen for the evaluation of total maintenance cost analysis. We adopted from the work of (Sa'ad et al., 2021), a 90% reliability threshold. All panels and other PV system components considered in this work are assumed to have similar ratings, therefore, maintenance action is illustrated for one (1) panel component which can be applied to many as considered.

Table 6: Maintenance parameters for solar energy

Component	Panel	DC wire	AC wire	Inverter	CM
Cost (NGN)	25,000	10,000	10,000	70,000	12,000
Time (tu)	0.3	0.2	0.2	0.3	15

The objective of the maintenance policy is to determine the optimal number of maintenance (N*) with minimal cost and maximal reliability. Having defined this in the algorithm, the optimal N obtained for all techniques applied are presented below. From the Tables, the optimal number of maintenances of 2 and 3 are obtained for the ANN and SVR methods at 114,717 NGN and 114,449 NGN respectively, which are graphically represented on figures 10 and 11.

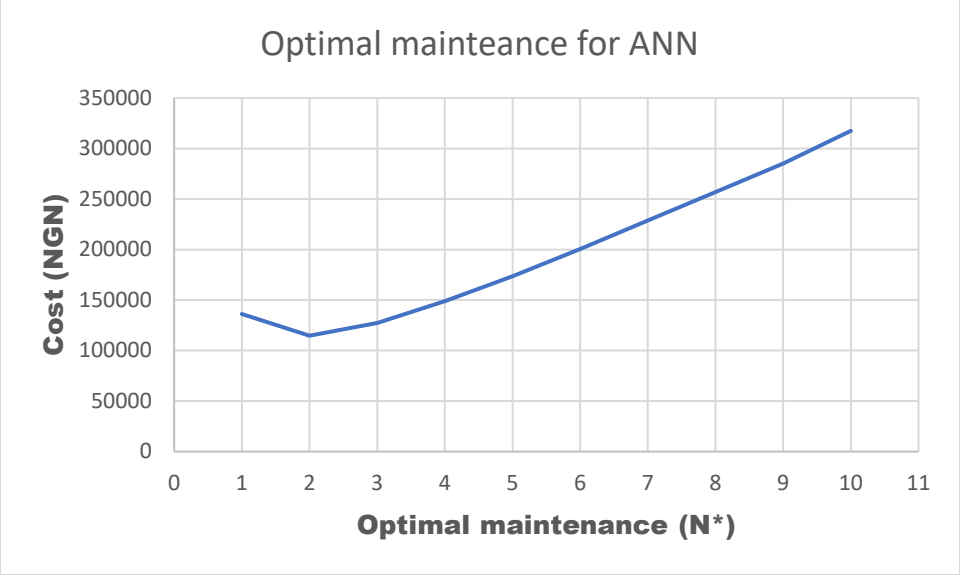

Figure 10: Optimal economic maintenance plan with the ANN technique

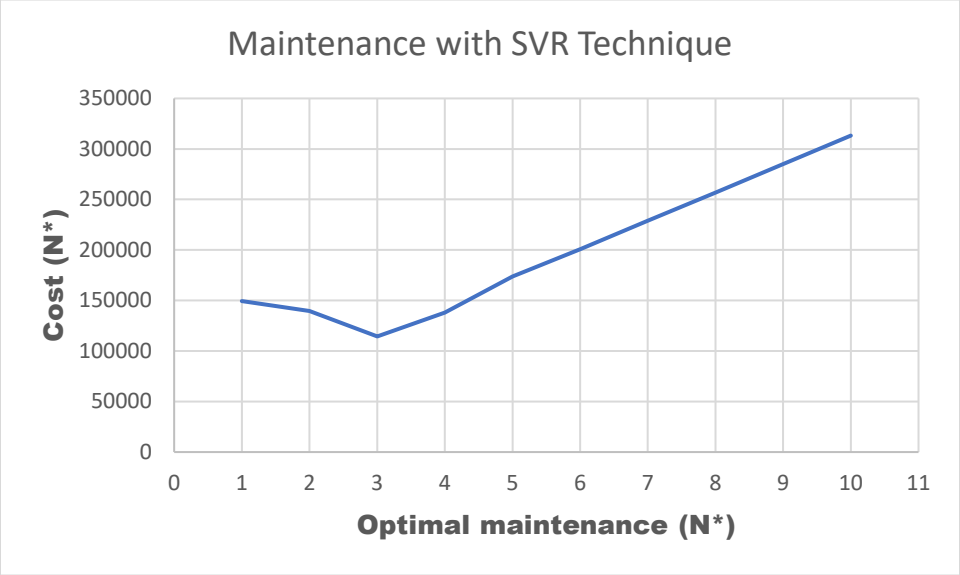

Figure 11: Optimal economic maintenance plan with the SVR technique

Components selected during each preventive maintenance period are shown on Tables 7 and 8. From Table 7, DC wire is the chosen component for replacement in the first maintenance period, while the panel and AC wire are selected during the second maintenance session. On table 8, inverter and DC wire are the chosen components during the first maintenance session. Again, inverter and AC wire are selected for the second

streak while only the panel is selected for the last maintenance streak.

Table 7: Components selected for maintenance during PM for ANN

Period	Panel	DC wire	AC wire	Inverter
1000	-	✓	-	-
2000	✓	-	✓	-

Table 8: Components selected for maintenance during PM for SVR

Period	Panel	DC wire	AC wire	Inverter
666	-	✓	-	✓
1334	-	-	✓	✓
2000	✓	-	-	-

Sensitivity analysis

To better understand the influence of some parameters on the system, the reliability threshold in this work was varied. For each of the techniques, the optimal number of maintenance as well as the cost implication is obtained for each varied reliability threshold and the result of which is presented on Table 9.

Table 9: Influence of reliability threshold on the optimal plan

Technique	R* (%)	N*	Cost (NGN)
ANN	80	2	129,941
	90	2	114,717
	95	2	133,249
SVR	80	2	120,459
	90	3	114,449
	95	3	149,057

From the above table, N* is seen to increase with increase in the reliability threshold. However, it has no influence on the cost as it is seen to fluctuate. For 80% reliability threshold, an optimal value of 2 is obtained for all the techniques. With this, the components selected during each maintenance streak is presented on Table 10. As shown on table, with the ANN, only the DC wire is to be replaced within the first maintenance whereas panel and AC wire are the selected components for the second streak. However, the SVR predicts DC wire, AC wire and the inverter all to be replaced during the first maintenance, and panel together with the inverter during the second maintenance period.

Table 10: Components selected for maintenance during PM (80%)

Technique	Period	Panel	DC wire	AC wire	Inverter
ANN	1000	-	✓	-	-

	2000	✓	-	✓	-
SVR	1000	-	✓	✓	✓
	2000	✓	-	-	✓

On Table 11, a reliability threshold of 95% is considered. Here, it is expected that 3 maintenances be performed using SVR and 2 using ANN. The components selected for each method is displayed on the table. With the ANN, inverter is not selected for replacement. The Dc wire is to be selected during the first maintenance, while panel and the AC wire during the second maintenance session. With the SVR, panel is to be replaced during the second and third maintenance exercises, DC wire during the first and third maintenance exercises, while AC wire during the second maintenance exercise and the inverter during the first and second maintenance exercises. Thus, this explains the inconsistency in obtaining the optimal cost.

Table 11: Components selected for maintenance during PM (95%)

Technique	Period (tu)	Panel	DC wire	AC wire	Inverter
ANN	1000	-	✓	-	-
	2000	✓	-	✓	-
SVR	666	-	✓	-	✓
	1334	✓	-	--	✓
	2000	✓	✓	-	-

Conclusion

The contribution of this work is the implementation of energy production policies and maintenance strategies for solar PV energy system subject to certain constraints. The main focus is on the development of new integrated production and maintenance strategies in the energy production system while ensuring maximum customer satisfaction. The developed models are subject to reliability constraints. Firstly, an optimization model based on machine learning techniques is developed. Its aim is to optimize the production system and determine the optimal number of components required; solar panels, and number of battery storage to satisfactorily supply the demand. The aim of the production planning was to determine the optimal cost of production by determining the optimal power produced as well as the optimal number of components that satisfy the demand per period. The novelty of this work is that it considers the cost of shortage and the loss cost in maintenance when planning the production such that economic losses associated to the production system is minimized.

The production planning optimization result is successfully integrated into the maintenance strategy to determine the optimal maintenance cost while ensuring maximum reliability is also achieved. Since the main aim of this work was to maximize reliability and availability which means minimizing maintenance down time, a priority selective imperfect maintenance strategy is adopted in order to select components for maintenance during preventive maintenance exercise. The selection was done under reliability threshold constraints such that at each preventive maintenance time, the reliability of each component is calculated and gauged with the threshold. When the reliability is found to fall below the threshold, that component is selected

for maintenance. We then developed an economic maintenance model that minimizes the economic cost of maintenance integrating reliability and production rate.

Findings showed that the ANN technique is the most suitable method for the optimization of the power plant because it presented the least optimal values thereby minimizing economic losses under maximum reliability. We also established that the higher the service rate, the more expensive the production cost. This is caused by increase in production rate as well as storage incorporation. It was also established that to ensure high standard of reliability, more maintenance is performed on the components due to increase in reliability thresholds. The increase in number of maintenances periods therefore, increases maintenance cost as well. For further research, hybridization of the renewable sources such as combining with wind energy, hydropower and biomass should be considered.

References

Adejumo, A. O., Suleiman, E. A., & Okagbue, H. I. (2017). Exploration of solar radiation data from three geo-political zones in Nigeria. *Data in Brief*, *13*, 60–68. https://doi.org/10.1016/j.dib.2017.05.017

Bahramirad, S., Reder, W., & Khodaei, A. (2012). Reliability-Constrained Optimal Sizing of Energy Storage System in a Microgrid. *IEEE Transactions on Smart Grid*, *3*(4), 2056–2062. https://doi.org/10.1109/TSG.2012.2217991

Bernal-Agustín, J. L., Dufo-López, R., & Rivas-Ascaso, D. M. (2006). Design of isolated hybrid systems minimizing costs and pollutant emissions. *Renewable Energy*, *31*(14), 2227–2244. https://doi.org/10.1016/j.renene.2005.11.002

Borowy B.S., and Salameh Z.M., 'Methodology for optimally sizing the combination of a battery bank and PV array in a wind/PV hybrid system', *IEEE Trans. Energy Convers.*, vol. 11, no. 2, pp. 367–375, Jun. 1996, doi: 10.1109/60.507648.

Capata, R. (2011). Lethe@-UDR1 Passenger Sedan Final Proposed Configuration. *Journal of Transportation Technologies*, *01*(04), 83–93. https://doi.org/10.4236/jtts.2011.14011

Cortes, C., & Vapnik, V. (1995). Support-vector networks. *Machine Learning*, *20*(3), 273–297. https://doi.org/10.1007/BF00994018

Diaf S., Diaf D., Belhamel M., Haddadi M., and Louche A. 'A methodology for optimal sizing of autonomous hybrid PV/wind system', Energy Policy, vol. 35, no. 11, pp. 5708–5718, Nov. 2007, doi: 10.1016/j.enpol.2007.06.020.

Dufo-López, R., Bernal-Agustín, J. L., & Contreras, J. (2007). Optimization of control strategies for stand-alone renewable energy systems with hydrogen storage. *Renewable Energy*, *32*(7), 1102–1126. https://doi.org/10.1016/j.renene.2006.04.013

Hanson, S. J. (1990). A stochastic version of the delta rule. *Physica D: Nonlinear Phenomena*, *42*(1–3), 265–272. https://doi.org/10.1016/0167-2789(90)90081-Y

Harrou, F., Saidi, A., Sun, Y., & Khadraoui, S. (2021). Monitoring of Photovoltaic Systems Using Improved Kernel-Based Learning Schemes. *IEEE Journal of Photovoltaics*, *11*(3), 806–818. https://doi.org/10.1109/JPHOTOV.2021.3057169

Hosseinalizadeh, R., Shakouri G, H., Amalnick, M. S., & Taghipour, P. (2016). Economic sizing of a hybrid (PV–WT–FC) renewable energy system (HRES) for stand-alone usages by an optimization-simulation model: Case study of Iran. *Renewable and Sustainable Energy Reviews*, *54*, 139–150. https://doi.org/10.1016/j.rser.2015.09.046

International Energy Agency. (2021). *World Energy Outlook 2021* (p. 386). https://iea.blob.core.windows.net/assets/4ed140c1-c3f3-4fd9-acae-789a4e14a23c/WorldEnergyOutlook2021.pdf

Li, J., Wei, W., & Xiang, J. (2012). A Simple Sizing Algorithm for Stand-Alone PV/Wind/Battery Hybrid Microgrids. *Energies*, *5*(12), 5307–5323. https://doi.org/10.3390/en5125307

Maatallah, T., Ghodhbane, N., & Ben Nasrallah, S. (2016). Assessment viability for hybrid energy

system (PV/wind/diesel) with storage in the northernmost city in Africa, Bizerte, Tunisia. *Renewable and Sustainable Energy Reviews*, *59*, 1639–1652. https://doi.org/10.1016/j.rser.2016.01.076

Mahani, K., Liang, Z., Parlikad, A. K., & Jafari, M. A. (2019). Joint Optimization of Operation and Maintenance Policies for Solar-Powered Microgrids. *IEEE Transactions on Sustainable Energy*, *10*(2), 833–842. https://doi.org/10.1109/TSTE.2018.2849318

Mellit, A., Kalogirou, S. A., Hontoria, L., & Shaari, S. (2009). Artificial intelligence techniques for sizing photovoltaic systems: A review. *Renewable and Sustainable Energy Reviews*, *13*(2), 406–419. https://doi.org/10.1016/j.rser.2008.01.006

Olatomiwa, L., Mekhilef, S., Shamshirband, S., Mohammadi, K., Petković, D., & Sudheer, C. (2015). A support vector machine–firefly algorithm-based model for global solar radiation prediction. *Solar Energy*, *115*, 632–644. ttps://doi.org/10.1016/j.solener.2015.03.015

Opiyo N.N. (2018) Different Storage-Focused PV-Based Mini-Grid Architectures for Rural Developing Communities', *Smart Grid Renew. Energy*, vol. 09, no. 05, pp. 75–99, 2018, doi: 10.4236/sgre.2018.95006.

Piller, S., Perrin, M., & Jossen, A. (2001). Methods for state-of-charge determination and their applications. *Journal of Power Sources*, *96*(1), 113–120. https://doi.org/10.1016/S0378-7753(01)00560-2

Realini, A. (2009). *Mean Time Before Failure of Photovoltaic modules*. 58.

Renewable Energy Market Update—*Outlook for 2021 and 2022*. (2021). 29.

Sa'ad, A., Hajej, Z., & Nyoungue, A. (2020). A day-ahead Multi-Approach Machine L earning Technique for Photovoltaic Power Forecasting. *2020 9th International Conference on Renewable Energy Research and Application (ICRERA)*, 257–262. https://doi.org/10.1109/ICRERA49962.2020.9242897

Sa'ad, A., Nyoungue, A. C., & Hajej, Z. (2021). Improved Preventive Maintenance Scheduling for a Photovoltaic Plant under Environmental Constraints. *Sustainability*, *13*(18), 10472. https://doi.org/10.3390/su131810472

Sa'ad, A., Nyoungue, A. C., & Hajej, Z. (2022). An integrated maintenance and power generation forecast by ANN approach based on availability maximization of a wind farm. *Energy Reports*, *8*, 282–301. https://doi.org/10.1016/j.egyr.2022.06.120

Tanesab, J., Parlevliet, D., Whale, J., & Urmee, T. (2018). Energy and economic losses caused by dust on residential photovoltaic (PV) systems deployed in different climate areas. *Renewable Energy*, *120*, 401–412. https://doi.org/10.1016/j.renene.2017.12.076

Voyant, C., Notton, G., Kalogirou, S., Nivet, M.-L., Paoli, C., Motte, F., & Fouilloy, A. (2017). Machine learning methods for solar radiation forecasting: A review. *Renewable Energy*, *105*, 569–582. https://doi.org/10.1016/j.renene.2016.12.095

Wang, Z., Xu, Z., Liu, B., Zhang, Y., & Yang, Q. (2022). A Hybrid Cleaning Scheduling Framework for Operations and Maintenance of Photovoltaic Systems. *IEEE Transactions on Systems, Man, and Cybernetics: Systems*, *52*(9), 5925–5936. https://doi.org/10.1109/TSMC.2021.3131031

Yang, H., Huang, K., King, I., & Lyu, M. R. (2009). Localized support vector regression for time series prediction. *Neurocomputing*, *72*(10–12), 2659–2669. https://doi.org/10.1016/j.neucom.2008.09.014

Zeroual, A., Harrou, F., & Sun, Y. (2021). Predicting road traffic density using a machine learning-driven approach. *2021 International Conference on Electrical, Computer and Energy Technologies (ICECET)*, 1–6. https://doi.org/10.1109/ICECET52533.2021.9698639.

Zhou W., Lou C., Li Z., Lu L., and Yang H., 'Current status of research on optimum sizing of stand-alone hybrid solar–wind power generation

systems', *Appl. Energy*, vol. 87, no. 2, pp. 380–389, Feb. 2010, doi: 10.1016/j.apenergy.2009.08.012.

Notation

$a_{corrosion}$ Corrosion coefficient constant under chemical influence
$a_{discoloration}$ Discoloration coefficient constant under chemical influence
AEC Available energy capacity of battery
$b_{corrosion}$ Corrosion coefficient constant under chemical influence
$b_{discoloration}$ Discoloration coefficient constant under chemical influence
$C_{corrosion}$ Corrosion coefficient for wires
C_{system} Cost index of the system
C_{cap} Capital cost of the system
C_{ope} Operational cost of the system
C_b Battery capacity
C_{t1} Cost of production
C_{t2} Cost of storage
C_{t3} Cost of shortage
C_{bat} Cost of purchasing battery
C_{pv} Cost of purchasing PV panel
C_{sell} Cost of selling 1 kW
DOD Depth of discharge
H Operation horizon
k Production period index (k = 1, 2, …H)
n_{series} Number of Series connections
n_{panels} Number of panels
n_{AC} Number of AC wires
n_{DC} Number of DC wires
$n_{inverter}$ Number of inverters
N Number of maintenances
N_{PV} Number of PV panels
P_b Power stored in the battery
P_k Power generation during period k
P_L Power load demand
P_S Power from solar energy
P_{max} Maximum power production level over the horizon
R*: Minimum required reliability threshold
$R(t)$ System reliability at t
$R_{equipment}$ Reliability function of equipment
R_{cause} Reliability function of cause of failure for a component
$R_{corrosion}$ Reliability function of corrosion
R_{DC} Reliability function of DC wire
R_{AC} Reliability function of AC wire
R_{wire} Reliability function of wire
R_{cut}: Reliability function of cut
$R_{inverter}$ Reliability function of inverter
R_{PV} Reliability function of PV system
R_{series} Reliability function of series
R_{panel} Reliability function of panel
$R_{junction}$ Reliability function of junction box
R_{glass} Reliability function of glass
$R_{byepass}$ Reliability function of bypass diode
R_{cell} Reliability function of cell
$R_{interconnect}$ Reliability function of interconnectors
$R_{delamination}$ Reliability function of delamination
$R_{hotspot}$ Reliability function of hotspot
$R_{discoloration}$ Reliability function of discoloration
R_{ribbon} Reliability function of ribbon
SOC State of charge of battery
TCb Total battery capacity of the system
V_b Voltage capacity of battery
μ_p Preventive maintenance time
μ_c Corrective maintenance time
$\varphi(N)$ Average number of failures
$\lambda_{cut-wire}$ Failure rate related to wire cut
$\lambda_{inverter}$ Inverter failure rate
$\lambda_{junction}$ Junction box failure rate
λ_{glass} Glass failure rate
$\lambda_{byepass}$ Bypass diode failure rate
λ_{cell} PV cell failure rate
$\lambda_{interconnect}$ Interconnection failure rate
$\lambda_{delamination}$ Delamination failure rate
$\lambda_{hotspot}$ hotspot failure rate
$\lambda_{discoloration}$ Discoloration failure rate
λ_{ribbon} Ribbon failure rate